Acta Polytechnica **65**(1):9–15, 2025
https://doi.org/10.14311/AP.2025.65.0009

THE TWO-POINT CORRELATION FUNCTION OF THE GRBS

Zsolt Bagoly[a, b]

[a] *University of Public Service, Department of Natural Sciences, 2 Ludovika tér, H-1083 Budapest, Hungary*
[b] *Eötvös University, Faculty of Science, Department of Physics of Complex Systems, Pázmány Péter sétány 1/A, H-1117 Budapest, Hungary*

correspondence: bagoly.zsolt@uni-nke.hu

Abstract. We analysed the spatial distribution of 542 GRBs with measured position and spectroscopic redshift up to 31 Aug 2022. Using kernel smoothing, we determined the GRB's Sky Exposure Function and used it in the generation of random catalogues. The spatial Two-Point Correlation Function for GRBs was determined by partitioning the data based on the origin of the redshift (afterglow or host galaxy).

The resulting $\xi(r)$ Two-Point Correlation functions remain below the 3σ noise level, suggesting no significant differences between the Two-Point Correlation functions of the random and real datasets.

Keywords: Data analysis, gamma-ray bursts.

1. Introduction

Gamma-ray bursts (GRBs) may be detected up to extermely high redshifts, making them excellent for studying large-scale structures. The Cosmological Principle states that the Universe is spatially homogeneous and isotropic on the large-scale. Usually we assume that GRBs follow the distribution of baryonic matter, so GRBs can test the distribution of baryonic matter in the Universe, particularly at large scales.

GRBs are assumed as one of the most powerful and extremely bright events the universe, caused by massive star bursts [1, 2] or binary compact object mergers [3]. Short GRBs are likely produced by the merger of compact objects, such as neutron stars or black holes, as proven by kilonova observations [4] and the GRB170817A event [5]. Long GRBs have been linked to collapsing huge star objects [6]. Therefore, long-duration GRBs are thought to arise from hypernovae in active star formation zones, indicating a close link between the two. GRBs are more abundant in low-metallicity, early star-forming areas of galaxies. Low metallicity influences stellar winds, allowing large stars to maintain more mass until exploding. GRBs may be viewed from a long distance, making them useful for studying star formation in the early cosmos.

The primary GRB groupings, notably the short and the long one, display distinct sky distributions, as demonstrated by the early *CGRO BATSE* observation of anisotropic detections [7–13]. The sky exposure is important because any association between the sky distribution and the physical parameters of the GRBs are quite interesting.

There is evidence for a third intermediate group [14–17], and the classification can be extended using different parameters and spectral models [18].

The sky distribution of 1 669 *Fermi/GBM* GRBs was used by [19] for the two-point angular correlation tests, closest neighbour, fractal dimension, dipole and quadrupole analysis, and binomial test. The results demonstrated that, with a probability of 99.98 %, short GRBs are dispersed anisotropically in the sky, but long GRBs exhibited no anisotropy. Using the two-point correlation function and closest neighbour tests, the large-scale homogeneous and isotropic distribution of 361 GRBs with known position and redshift was verified in [20]. [21] used conditional density and pairwise distance techniques to estimate a fractal dimensionality[1] of $D = 2.55$ on scales of 2–6 Gpc.

[22] examined the isotropy of the sky distribution of 2 626 GRBs from the FERMI-GBM archive. For both the long and short GRBs, the applied two-point angular correlation function was unable to identify any statistical anisotropy due to the significant positional uncertainty in the locations. Using prompt and afterglow parameters, [23] examined several intrinsic aspects of 6 289 GRBs and looked for relationships between the parameters and the GRBs' categorisation.

[24] tested the correlation between GRBs' sky locations, durations, fluences, and peak fluxes observed in various energy ranges using the *Fermi GBM* GRB observations. [25] added the *BATSE* and *Swift BAT* GRBs to the data. This study revealed no relationship between the GRBs' physical characteristics and their sky locations. The relationship between the durations of the GRBs and redshifts/radial distances was recently examined by [26], who also discovered no link between them.

These findings support the theory that the physical characteristics of GRBs are unaffected by their location throughout the universe.

Data from 542 GRBs up to 31 August 2022, were used in this analysis. The GRBs were mostly observed by NASA's *Swift* and/or *Fermi* spacecraft, and the

[1] Fractal dimensionality describes the complexity and scaling properties of fractals, which are self-similar patterns exhibiting self-similarity or hierarchical structure.

spectroscopic redshifts were obtained with a variety of redshift observations. The primary data source was Index (GRBOX) database [27], however, the GCN data were also directly used. Jochen Greiner's publicly accessible dataset [28] was cross-checked to the data as well. Since photometric redshifts and redshift estimations have significant errors that reach several hundred of Mpcs, the study exclusively employed spectroscopic redshifts only. A distinction was made according to the origin of the redshift (optical afterglows or host galaxy measurements) as the host galaxies' distances are lower due to observational constraints.

2. The two-point correlation function

A statistical technique used in cosmology to measure the large-scale features and the spatial distribution of galaxies and other sources is the two-point correlation function. It quantifies the extra likelihood of discovering two sources spaced apart by a specific distance when compared to a random distribution.

The $\xi(r)$ two-point correlation function, is defined as the excess probability over random of finding two sources separated by a distance r:

$$dP = n[1 + \xi(r)]dV, \tag{1}$$

where

dP is the probability of finding a pair of galaxies separated by r,

n is the mean number density of galaxies,

dV is the volume element.

At a distance r, the distribution of galaxies is random if $\xi(r) = 0$. When $\xi(r)$ is positive, it indicates clustering by a larger likelihood of finding galaxies separated by r than at random. If $\xi(r)$ is negative then there is a lesser likelihood than random to locate galaxies separated by r, suggesting voids. Since the two-point correlation function is the inverse Fourier transform of the power spectrum, both forms characterise point distributions similarly.

3. Large-scale anomalies

3.1. Compton gamma-ray observatory observations

The *Compton Gamma-ray Observatory BATSE* dataset [29] has been the subject of numerous studies, including the first indirect observational proof for the cosmological origin of GRBs. After the first two years of *BATSE* observations, the observed GRBs showed an almost isotropic distribution without any concentration around the Galactic plane [30]. The results strengthened the cosmological origin model of the sources. Using angular positional measurements from the *BATSE* experiment, [7] found that the sky distributions of short and long GRBs are different, with a probability of 99.97 %. The anisotropic sky exposure was considered, and the effects were found to be small. However, this anisotropic sky exposure complicated the detailed statistics.

The short-distance sky distribution of GRBs is anisotropic, with $p = 0.00016$ level [8, 31]. However, due to the *BATSE's* anisotropic sky exposure, the Two-Point Angular Correlation Function is not uniform too. The effects of sky exposure are small, but the non-uniformity of the sky exposure complicates detailed statistics, indicating that it should be specifically addressed [32].

In [10], the distribution of intermediate GRB data was analysed using a modified *BATSE* count-in-cell approach. The results indicate that the distribution is not isotropic with a 99.3 % confidence level. [11] employed spherical harmonics to study the angular distribution of the intermediate group, demonstrating inherent anisotropy with a 97 % significance level. In [12], short bursts exhibited a greater 99.99 % significance level of anisotropy, whereas intermediate bursts had a lower 99.89 % significance level. [33] discovered the association between short GRBs and galaxies' locations in the local universe at a 99.9 % significance level. In [13], the *BATSE* data revealed that short GRBs depart considerably from complete randomness at a 99.90–99.98 % level, whereas the intermediate group exhibited a lesser but still significant deviation at a 98.51 % level from isotropy.

3.2. Large-scale structures using the spectroscopic redshift data

In [34], a large GRB cluster at $z \approx 2$ was discovered in the direction of Hercules and Corona Borealis. The study examined the spatial distribution of 283 GRBs with different redshifts. The sample was divided by z, with the assumption that sky exposure is independent of radial distribution. The dataset was analysed using the k^{th} nearest neighbour and bootstrap point radius techniques. Nearest-neighbour investigations [35] support the existence of this huge, loose GRB cluster in the redshift range $1.6 < z \leq 2.1$, with a $p = 1.6 \times 10^{-4}$ likelihood. Additional data and analysis corroborated the discovery of additional GRBs with measured redshifts [36]. The structure's actual nature is uncertain.

[37] examined the k^{th} nearest neighbour in the GRB sample, after the detection of the Hercules-Corona Borealis Great Wall. To estimate the spatial density of GRBs, instead of the redshift space slices, it used k^{th} Next Neighbour Statistics. The analysis of $k = 8, 10, 12$, and 14 revealed the Giant GRB Ring, consisting of 9 GRBs with an angular major/minor diametre of 43°/30° at a distance of $\approx 2\,770$ Mpc in the $0.78 < z < 0.86$ redshift range, with a probability of 2×10^{-6} of being a random fluctuation [38].

4. The sky exposure function

The redshift-determined GRB detection probability in the sky is a multi-parameter event that relies on

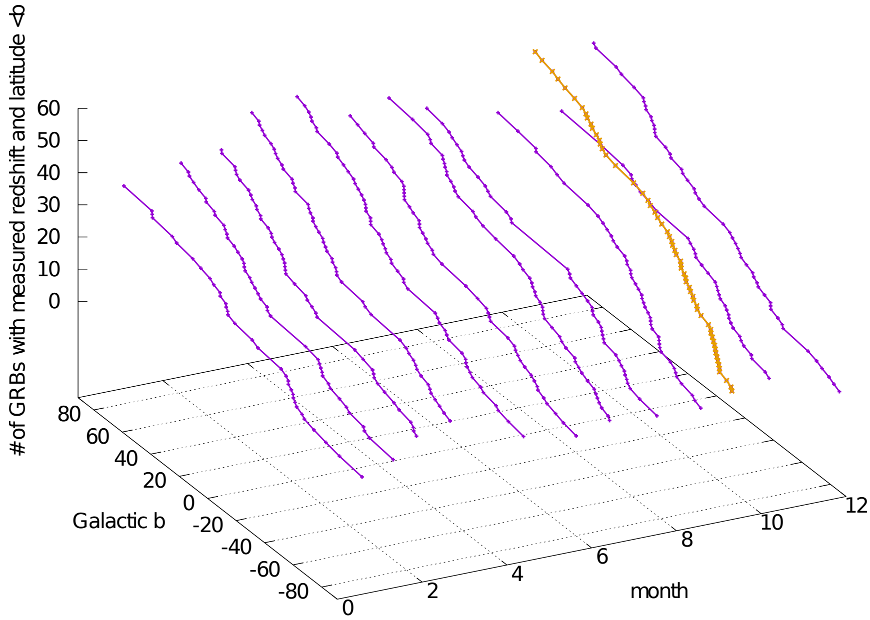

FIGURE 1. Monthly variances of the cumulative distribution of the successful spectroscopic observations in the current sample. Dedicated optical campaigns in October in the last few years are raising the orange line above the expectation – this is a clear outlier.

different space instrument trigger, and detection circumstances as well as the optical follow-up protocol. Satellite pointing records can be used to generate the most basic sky exposure models, however this is not very practical owing to both technological and human considerations. The information available indicates that developing a robust model for selection effects, encompassing the influence of galactic extinction and other optical observational restrictions and effects, is essentially unfeasible.

In Figure 1 the yearly variances of the spectroscopic observations are shown. The cumulative number density is plotted for each month against the galactic latitude. One can observe the yearly changes with the exception of October.

With the exception of the afterglow's October distribution, the distribution of afterglow and host galaxy measurements roughly follow the same pattern with very comparable annual modulation. The additional 10–15 observations are likely caused by optical campaigns in the last few years.

Since the synthetic method is not practical, we must calculate the empirical Sky Exposure Function using simply the observational data. This is not in contradiction since the dataset-averaged sky detection probability can be estimated, provided that the sky distribution is assumed to be independent of redshift [20, 39].

5. Kernel smoothing

A basic non-parametric technique for estimating regression and probability density functions in statistics is kernel smoothing. Kernel smoothing is versatile and broadly applicable, as it avoids assuming a specific underlying distribution for the data, unlike parametric approaches. Selecting the kernel function is frequently less important than selecting the bandwidth. The Gaussian, Epanechnikov, and uniform kernels are frequently used kernel functions [40].

Using several methods, the optimum empirical Sky Exposure Function was rebuilt from the point distribution in [39]. On a random field that imitated the *Swift's* exposure map, the effectiveness of the fixed and adaptive width Gaussian kernel, the Delaunay Tessellation Field Estimator [41], and the Voronoi Diagram Field Estimator techniques [42] were tested. The fixed-width Gaussian kernel smoothing was shown to be the best approach for both estimating the exposure map and figuring out the ideal width.

Kernel-based techniques were used in [20, 43, 44] to reconstruct the empirical Sky Exposure Function of the GRBs. To get the empirical Sky Exposure Function, we smoothed the current GRB data using Gaussian kernels. The ideal kernel-smoothed Sky Exposure Function is shown in Figure 2. The galactic disc is visible, and the difference between the minimum and maximum is a factor of $\gtrsim 5$. The typical 20–40° range [39] contains the optimal kernel sizes for the usual few hundreds of GRBs, which are obviously larger than the galactic optical extinction range width. As a result, kernels will provide a smoother sky exposure than the real ones, which will reduce the statistical power of detecting structures close to and below the kernel size.

6. The spatial Two-point Correlation Function

The spatial Two-point Correlation Function $\xi(r)$ was determined using the earlier estimated empirical Sky

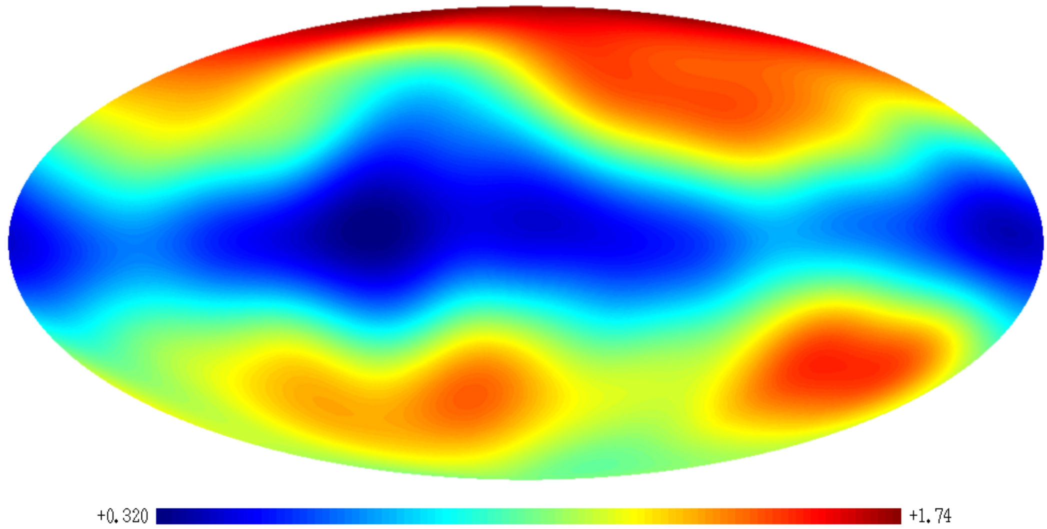

Figure 2. The empirical Sky Exposure Function of the GRBs reconstructed with optimal Gaussian smoothing, FWHM = 2221'. Normalised units are applied.

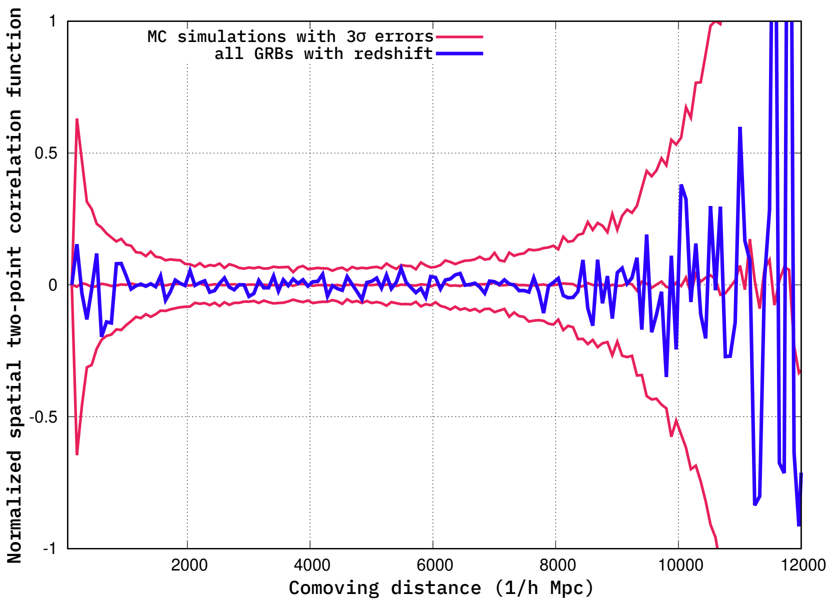

Figure 3. The spatial two-point correlation function for all GRBs.

Exposure Function and the radial (comoving distance) distribution of the data.

The simple Peebles-Hauser's estimator [45] of the two-point correlation function $\xi(r)$ is sometimes biased and not well suitable for edge effects and survey boundaries, particularly when there is a large-scale structure present. Therefore, the Landy-Szalay estimator [46] was applied as the most effective technique for a lower observational probability and known partial vignetting:

$$\xi(r) = \frac{DD(r) - 2DR(r) + RR(r)}{RR(r)}, \qquad (2)$$

where $DD(r)$, $RR(r)$ and $DR(r)$ are the count of pairs between the data-data, random-random and data and random samples at separation r. The Landy-Szalay estimator minimises variance compared to other estimators and corrects for edge effects and the survey's irregular geometry.

For the computations, we used 10 000 random points. To generate Monte Carlo simulations, we additionally employed 100 synthetic datasets with the same marginal distributions as the original data. The Poissonian errors in the computations were found using the obtained $\xi(r)$'s from the random datasets.

A major source of the noise at both ends of the $\xi(r)$ arises from the lower counts, especially the $RR(r)$ in the denomator causes big errorbars. We created here bin sizes which contain approximately an equal number of random points. Hence, by aggregating the number of events in the bins at both ends, it will slightly reduce the noise in the $RR(r)^{-1}$ function. Still, at large distances, the error bars are quite large.

The $\xi(r)$ of the whole dataset is displayed in Figure 3, with the mean value and the $\pm 3\sigma$ errors.

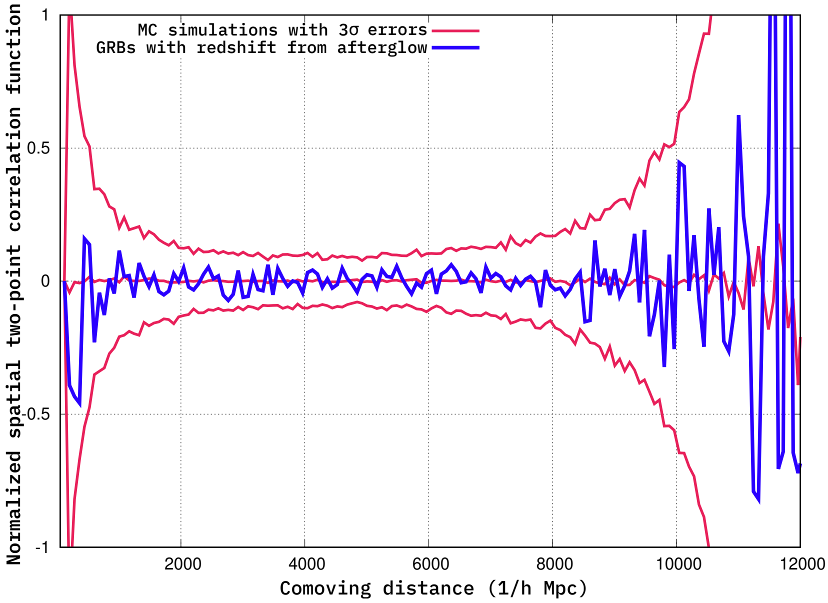

FIGURE 4. The spatial two-point correlation function for GRBs with z from afterglows.

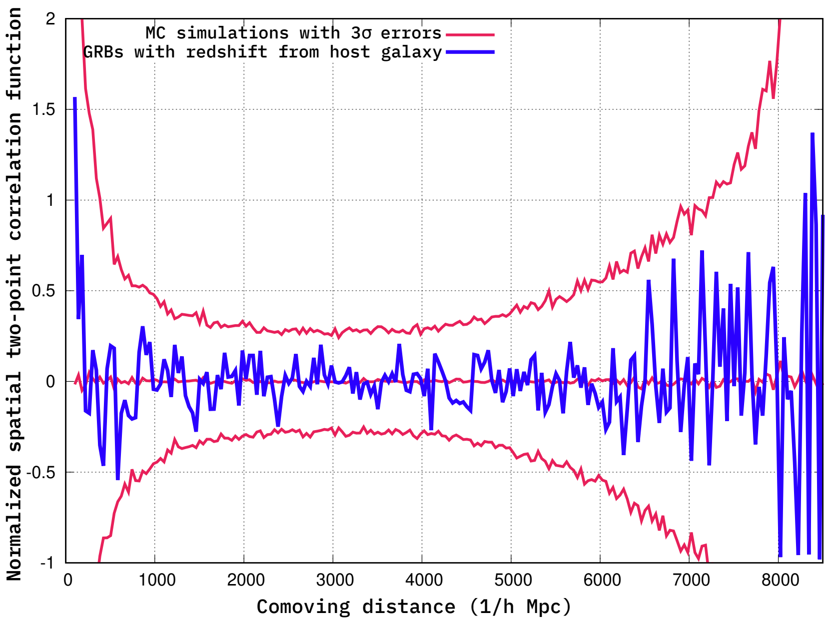

FIGURE 5. The spatial two-point correlation function for GRBs with z from host galaxies.

The $\pm 3\sigma$ error lines indicate noise, and the mean of the approximately 100 synthetic datasets should be 0. For the real GRB distribution, the ξ values fall within the errors, and there is no signal at the $\pm 3\sigma$ level.

We repeated the $\xi(r)$ calculation for the afterglow and host galaxy subsets separately. The matching $\xi(r)$ functions are shown in Figures 4 and 5, along with the related $\pm 3\sigma$ lines, respectively. The GRB $\xi(r)$ values are the same within the 3σ errors in both situations.

All the resulting $\xi(r)$ two-point correlation functions are consistent with zero. Considering the observations detailed in Section 3 it can indicate that the χ^2 optimal kernel width over-smooths the real Sky Exposure Function.

Our results are similar to those of [20, 26], although we used a slightly larger number of events ($n = 542$ versus $n = 361$ and 533) with a correspondingly smaller kernel size. It is important to note that a smoothed sky exposure compared to the actual sky exposure reduces statistical power, making it less effective for detecting structures near or below the kernel size. The new quasi-optimisation of the bin sizes for $RR(r)$ reduced some of the noise at the extremes, resulting in a slightly lower error bars. However, the $\xi(r)$ signal remained below the 3σ level, consistent with previous studies.

ACKNOWLEDGEMENTS

The author thanks the Hungarian TKP2021-NVA-16 and TKP2021-NKTA-64 programs for their support.

References

[1] S. E. Woosley. Gamma-ray bursts from stellar mass accretion disks around black holes. *The Astrophysical Journal* **405**:273, 1993. https://doi.org/10.1086/172359

[2] S. E. Woosley, J. S. Bloom. The supernova gamma-ray burst connection. *Annual Review of Astronomy and Astrophysics* **44**:507–556, 2006. https://doi.org/10.1146/annurev.astro.43.072103.150558

[3] E. Berger. Short-duration gamma-ray bursts. *Annual Review of Astronomy and Astrophysics* **52**:43–105, 2014. https://doi.org/10.1146/annurev-astro-081913-035926

[4] N. R. Tanvir, A. J. Levan, A. S. Fruchter, et al. A 'kilonova' associated with the short-duration γ-ray burst GRB 130603B. *Nature* **500**(7464):547–549, 2013. https://doi.org/10.1038/nature12505

[5] A. von Kienlin, P. Veres, O. J. Roberts, et al. Fermi-GBM GRBs with characteristics similar to GRB 170817A. *The Astrophysical Journal* **876**(1):89, 2019. https://doi.org/10.3847/1538-4357/ab10d8

[6] S. Woosley, J. Bloom. The supernova–gamma-ray burst connection. *Annual Review of Astronomy and Astrophysics* **44**:507–556, 2006. https://doi.org/10.1146/annurev.astro.43.072103.150558

[7] L. G. Balázs, A. Mészáros, I. Horváth. Anisotropy of the sky distribution of gamma-ray bursts. *Astronomy & Astrophysics* **339**:1–6, 1998. https://doi.org/10.48550/arXiv.astro-ph/9807006

[8] D. B. Cline, C. Matthey, S. Otwinowski. Study of very short gamma-ray bursts. *The Astrophysical Journal* **527**(2):827–834, 1999. https://doi.org/10.1086/308094

[9] M. Magliocchetti, G. Ghirlanda, A. Celotti. Evidence for anisotropy in the distribution of short-lived gamma-ray bursts. *Monthly Notices of the Royal Astronomical Society* **343**(1):255–258, 2003. https://doi.org/10.1046/j.1365-8711.2003.06657.x

[10] A. Mészáros, Z. Bagoly, I. Horváth, et al. A remarkable angular distribution of the intermediate subclass of gamma-ray bursts. *The Astrophysical Journal* **539**(1):98–101, 2000. https://doi.org/10.1086/309193

[11] A. Mészáros, Z. Bagoly, R. Vavrek. On the existence of the intrinsic anisotropies in the angular distributions of gamma-ray bursts. *Astronomy & Astrophysics* **354**:1–6, 1999. https://doi.org/10.48550/arXiv.astro-ph/9912037

[12] V. F. Litvin, S. A. Matveev, S. V. Mamedov, V. V. Orlov. Anisotropy in the sky distribution of short gamma-ray bursts. *Astronomy Letters* **27**(7):416–420, 2001. https://doi.org/10.1134/1.1381609

[13] R. Vavrek, L. G. Balázs, A. Mészáros, et al. Testing the randomness in the sky-distribution of gamma-ray bursts. *Monthly Notices of the Royal Astronomical Society* **391**(4):1741–1748, 2008. https://doi.org/10.1111/j.1365-2966.2008.13635.x

[14] A. Balastegui, P. Ruiz-Lapuente, R. Canal. Reclassification of gamma-ray bursts. *Monthly Notices of the Royal Astronomical Society* **328**(1):283–290, 2001. https://doi.org/10.1046/j.1365-8711.2001.04888.x

[15] I. Horváth, L. G. Balázs, Z. Bagoly, et al. A new definition of the intermediate group of gamma-ray bursts. *Astronomy & Astrophysics* **447**(1):23–30, 2006. https://doi.org/10.1051/0004-6361:20041129

[16] T. Chattopadhyay, R. Misra, A. K. Chattopadhyay, M. Naskar. Statistical evidence for three classes of gamma-ray bursts. *The Astrophysical Journal* **667**(2):1017–1023, 2007. https://doi.org/10.1086/520317

[17] D. Pérez-Ramírez, A. de Ugarte Postigo, J. Gorosabel, et al. Detection of the high z GRB 080913 and its implications on progenitors and energy extraction mechanisms. *Astronomy & Astrophysics* **510**:A105, 2010. https://doi.org/10.1051/0004-6361/200811151

[18] I. Horváth, J. Hakkila, Z. Bagoly, et al. Multidimensional analysis of Fermi GBM gamma-ray bursts. *Astrophysics and Space Science* **364**(6):105, 2019. https://doi.org/10.1007/s10509-019-3585-1

[19] M. Tarnopolski. Testing the anisotropy in the angular distribution of Fermi/GBM gamma-ray bursts. *Monthly Notices of the Royal Astronomical Society* **472**(4):4819–4831, 2017. https://doi.org/10.1093/mnras/stx2356

[20] Z. Bagoly, I. Horváth, J. Hakkila, L. V. Tóth. Anomalies in the GRBs' distribution. *Proceedings of the International Astronomical Union* **11**(S319):2–2, 2015. https://doi.org/10.1017/S1743921315010182

[21] S. I. Shirokov, A. A. Raikov, Y. V. Baryshev. Spatial distribution of gamma-ray burst sources. *Astrophysics* **60**(4):484–496, 2017. https://doi.org/10.1007/s10511-017-9500-y

[22] U. Andrade, C. A. P. Bengaly, J. S. Alcaniz, S. Capozziello. Revisiting the statistical isotropy of GRB sky distribution. *Monthly Notices of the Royal Astronomical Society* **490**(4):4481–4488, 2019. https://doi.org/10.1093/mnras/stz2754

[23] F. Wang, Y.-C. Zou, F. Liu, et al. A comprehensive statistical study of gamma-ray bursts. *The Astrophysical Journal* **893**(1):77, 2020. https://doi.org/10.3847/1538-4357/ab0a86

[24] J. Řípa, A. Shafieloo. Testing the isotropic universe using the gamma-ray burst data of Fermi/GBM. *The Astrophysical Journal* **851**(1):15, 2017. https://doi.org/10.3847/1538-4357/aa9708

[25] J. Řípa, A. Shafieloo. Update on testing the isotropy of the properties of gamma-ray bursts. *Monthly Notices of the Royal Astronomical Society* **486**(3):3027–3040, 2019. https://doi.org/10.1093/mnras/stz921

[26] I. Horvath, I. I. Racz, Z. Bagoly, et al. Does the GRB duration depend on redshift? *Universe* **8**(4):221, 2022. https://doi.org/10.3390/universe8040221

[27] D. Perley. GRBOX: Gamma-ray burst online index. [2023-06-01]. https://sites.astro.caltech.edu/grbox/grbox.php

[28] J. Greiner. Gamma-ray burst: Afterglows, 2006. [2023-06-01]. https://www.mpe.mpg.de/~jcg/grb.html

[29] NASA's High energy astrophysics science archive research center. BATSEGRB – CGRO/BATSE gamma-ray burst catalog, 2024. [2023-06-01]. https://heasarc.gsfc.nasa.gov/w3browse/all/batsegrb.html

[30] C. A. Meegan, G. J. Fishman, R. B. Wilson, et al. Spatial distribution of γ-ray bursts observed by BATSE. *Nature* **355**(6356):143–145, 1992. https://doi.org/10.1038/355143a0

[31] D. B. Cline. *The role of neutrinos, strings, gravity, and variable cosmological constant in elementary particle physics*, chap. Primordial black holes and the asymmetrical distribution of short GRB events, pp. 157–168. Springer US, Boston, USA, 2001. https://doi.org/10.1007/0-306-47116-7_14

[32] X. Chen, J. Hakkila. The two-point angular correlation function and BATSE sky exposure. *AIP Conference Proceedings* **428**(1):149–153, 1998. https://doi.org/10.1063/1.55312

[33] N. R. Tanvir, R. Chapman, A. J. Levan, R. S. Priddey. An origin in the local Universe for some short γ-ray bursts. *Nature* **438**(7070):991–993, 2005. https://doi.org/10.1038/nature04310

[34] I. Horváth, J. Hakkila, Z. Bagoly. Possible structure in the GRB sky distribution at redshift two. *Astronomy and Astrophysics* **561**:L12, 2014. https://doi.org/10.1051/0004-6361/201323020

[35] I. Horváth, Z. Bagoly, J. Hakkila, L. V. Tóth. New data support the existence of the Hercules-Corona Borealis Great Wall. *Astronomy & Astrophysics* **584**:A48, 2015. https://doi.org/10.1051/0004-6361/201424829

[36] I. Horvath, D. Szécsi, J. Hakkila, et al. The clustering of gamma-ray bursts in the Hercules-Corona Borealis Great Wall: the largest structure in the Universe? *Monthly Notices of the Royal Astronomical Society* **498**(2):2544–2553, 2020. https://doi.org/10.1093/mnras/staa2460

[37] L. G. Balázs, Z. Bagoly, J. E. Hakkila, et al. A giant ring-like structure at $0.78 < z < 0.86$ displayed by GRBs. *Monthly Notices of the Royal Astronomical Society* **452**(3):2236–2246, 2015. https://doi.org/10.1093/mnras/stv1421

[38] L. G. Balázs, L. Rejtő, G. Tusnády. Some statistical remarks on the giant GRB ring. *Monthly Notices of the Royal Astronomical Society* **473**(3):3169–3179, 2017. https://doi.org/10.1093/mnras/stx2550

[39] Z. Bagoly, L. G. Balázs, I. Horváth, et al. The GRB's sky exposure function. In *Proceedings of Swift: 10 Years of Discovery – PoS(SWIFT 10)*, vol. 233, p. 60. 2015. https://doi.org/10.22323/1.233.0060

[40] B. W. Silverman. *Density estimation for statistics and data analysis*. Chapman and Hall/CRC, 1986.

[41] W. E. Schaap, R. van de Weygaert. Continuous fields and discrete samples: Reconstruction through Delaunay tessellations. *Astronomy & Astrophysics* **363**:L29–L32, 2000. https://doi.org/10.48550/arXiv.astro-ph/0011007

[42] A. Okabe, B. Boots, K. Sugihara, S. N. Chiu. *Spatial tessellations: Concepts and applications of Voronoi diagrams*. Wiley Series in Probability and Statistics. Wiley, USA, 2nd edn., 2009.

[43] M.-H. Li, H.-N. Lin. Testing the homogeneity of the Universe using gamma-ray bursts. *Astronomy & Astrophysics* **582**:A111, 2015. https://doi.org/10.1051/0004-6361/201525736

[44] T. N. Ukwatta, P. R. Woźniak, N. Gehrels. Machine-z: rapid machine-learned redshift indicator for Swift gamma-ray bursts. *Monthly Notices of the Royal Astronomical Society* **458**(4):3821–3829, 2016. https://doi.org/10.1093/mnras/stw559

[45] A. J. S. Hamilton. Toward better ways to measure the galaxy correlation function. *The Astrophysical Journal* **417**:19, 1993. https://doi.org/10.1086/173288

[46] S. D. Landy, A. S. Szalay. Bias and variance of angular correlation functions. *The Astrophysical Journal* **412**:64, 1993. https://doi.org/10.1086/172900